Korean J. Chem. Eng., **15**(1), 56-63 (1998)

MODELING OF SiO_2 CVD FROM TEOS/OZONE IN A SEPARATE-GAS-INJECTION REACTOR

Eui Jung Kim† **and William N. Gill***

Department of Chemical Engineering, University of Ulsan, San 29, Moogeodong, Namku, Ulsan 680-749, Korea
*Department of Chemical Engineering, Rensselaer Polytechnic Institute, Troy, New York 12180-3590, U.S.A.
(Received 21 July 1997 • accepted 12 November 1997)

Abstract – A mathematical model has been developed to study the chemical vapor deposition of SiO_2 from TEOS and ozone in a cold-wall separate-gas-injection reactor related to the commercial Watkins-Johnson 7000. The model employs the kinetic scheme proposed previously by Kim and Gill. Control-volume-based finite difference methods are used to solve for the two-dimensional fluid velocity, temperature, and concentration distributions. The model successfully describes experimental data of film thickness profiles available. We systematically investigate the dependence of deposition rate on operating conditions including O_3/TEOS ratio, reactant flow rate, and injector-wafer spacing. The predicted results indicate that a high TEOS flow rate and an O_3/TEOS ratio of around 30 are preferable for obtaining high deposition rates and good film quality.

Key words: *CVD, SiO_2 Film, TEOS/Ozone Process, Separate-Gas-Injection*

INTRODUCTION

Silicon dioxide films have played a key role as dielectrics for very large scale integrated (VLSI) devices. Advanced chemical vapor deposition (CVD) dielectric films have to be of high quality, represented by such measures as conformal step coverage, high density, low deposition temperature, low film stress, high moisture resistance, and high breakdown voltage. The conventional silane-based CVD process producing SiO_2 films often incurs poor step coverage, particle generation, and high stress. TEOS (tetraethoxysilane) has gained increasing attention as an organometallic precursor for depositing SiO_2 films because of yielding high film quality and superior step coverage. It decomposes thermally at temperatures above 600 °C, which are too high for applying to interlayer dielectric films. Silicon dioxide films can be deposited at sufficiently low temperatures using plasma-enhanced CVD [Park et al., 1996; Jeon et al., 1997]. However, poor step coverage and carbon contamination remain as drawbacks [Chin and Van de Ven, 1988]. TEOS/ozone CVD processes have attracted attention as one of the methods to deposit SiO_2 films at low temperatures below 500 °C with excellent step coverage, low film stress, and low particle formation during deposition.

Nguyen et al. [1990] observed that TEOS/ozone films deposited at 50 torr were porous but extremely conformal when compared to plasma films. Several studies from Japan [Nishimoto et al., 1989; Fujino et al., 1990; Ikeda et al., 1990] showed that the atmospheric pressure CVD (APCVD) process using TEOS/ozone produces high quality dielectric films with excellent step coverage. They argued that this APCVD process is sufficient for meeting the requirements for ultra large scale integrated (ULSI) technology. Li et al. [1993] performed gap filling studies and found that oxide films of low ozone concentration processes are conformal. Kim and Gill [1994] developed a detailed kinetic model for the TEOS/ozone process that successfully explains experimental data over a wide range of operating conditions. Recently, Shareef et al. [1995] showed that a subatmospheric CVD (SACVD) TEOS/ozone process is capable of high deposition rate, good film quality, and excellent step coverage.

Most of the previous work on TEOS/ozone process reported in the literature has been done using a reactor configuration in which the reactants are mixed before entering the chamber from the showerhead like the Applied Materials (AM) 5000. In this article, we present a mathematical model to explore the TEOS/ozone CVD process based on a configuration related to the commercial Watkins-Johnson (WJ) 7000 in which TEOS and ozone are injected separately into the CVD chamber. We consider here film thickness profiles on a stationary wafer whose experimental data are available. The present model employs TEOS/ozone kinetic mechanisms proposed by Kim and Gill [1994]. Numerical simulations are performed to investigate the dependence of deposition rate on operating conditions including O_3/TEOS ratio, reactant flow rate, and injector-wafer spacing.

WJ 7000 CVD REACTOR CONFIGURATION

Fig. 1 depicts a schematic diagram of the WJ 7000 CVD reactor that is operated under atmospheric pressure. As shown in Fig. 1, the gas injector, which is maintained at 60 °C, dispenses five streams of gas over the wafer. The inner port carries TEOS diluted in nitrogen, nitrogen flows through the separator port, and the outer port carries ozonated oxygen. One can easily realize that the TEOS and ozone streams are sep-

†To whom all correspondence should be addressed.
E-mail: ejkim@uou.ulsan.ac.kr

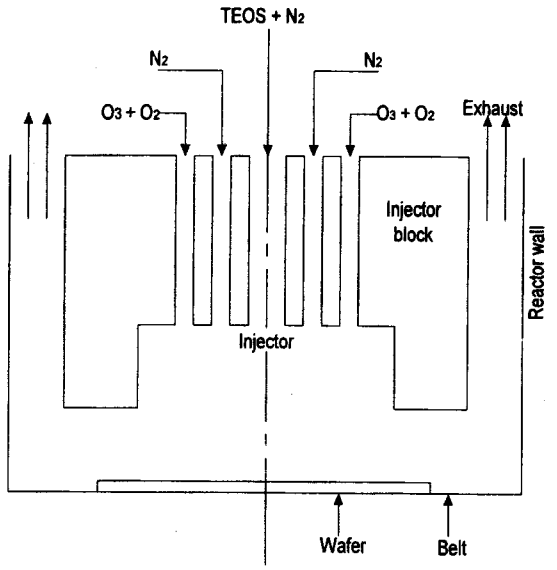

Fig. 1. Schematic diagram of Watkins-Johnson 7000 configuration.

arated by an inert gas "blanket" in order to reduce gas phase reactions in the WJ CVD chamber, unlike the AM 5000 in which the gas reactants are mixed before being injected into the chamber. The exit slots of the injector are quite small (1 mm each) but the chamber itself is fairly large (about 1.5 cm high by several cm wide, and typically 40 cm deep).

To obtain uniform films the WJ 7000 system employs a metal mesh belt that carries wafers beneath a linear gas injector. The belt rides on an Inconel floor that is resistively heated from below. In commercial operation the wafers move slowly under the gas injectors so that each portion of the wafer surface is exposed to the same conditions for the same amount of time, which results in a uniform film (typically nonuniformity below 2%), and the degree of uniformity is relatively independent of wafer size. However, deposition rates obtained from the WJ 7000 configuration seem to be unsatisfactory and remain to be raised. Experimental data are available on stationary wafers called "static prints" [Li et al., 1993]. We consider in this work "static prints" to better understand the behavior of film thickness profiles observed by Li et al. [1993] and investigate numerically the effect of operating conditions on deposition rate in an effort to improve deposition rate and film quality obtained from the WJ 7000.

MATHEMATICAL MODEL

The mathematical model for the TEOS/ozone CVD process in the WJ 7000 system includes a set of partial differential equations describing fluid flow, heat transfer, mass transport of chemical species, and chemical reactions in the gas phase and on the wafer surface. Some simplifying assumptions are applied to the CVD system considered in this work: (i) A steady state situation is considered. (ii) A laminar flow is assumed. (iii) The gas mixture is ideal. (iv) Reactants such as TEOS and ozone are highly diluted in the carrier gas. (v) Energy contributions caused by heats of reactions are negligible. The last two assumptions imply that the flow and temperature calculations are decoupled from the species balance. With these assumptions above, we have the governing equations that follow.

1. Governing Equations

In rectangular coordinates the continuity equation is given by

$$\frac{\partial \rho u}{\partial x} + \frac{\partial \rho v}{\partial y} = 0 \tag{1}$$

where ρ is the density of the gas mixture, u is the longitudinal velocity, v is the lateral velocity, x is the longitudinal coordinate, and y is the lateral coordinate. The stream function, Ψ, is defined as

$$\rho u = \frac{\partial \Psi}{\partial y}, \quad \rho v = -\frac{\partial \Psi}{\partial x} \tag{2}$$

The momentum equations governing the motion of the gas are written as

x-component:

$$\rho\left(u\frac{\partial u}{\partial x} + v\frac{\partial u}{\partial y}\right) = -\frac{\partial P}{\partial y} + \frac{\partial}{\partial x}\left(\mu\frac{\partial u}{\partial x}\right) + \frac{\partial}{\partial y}\left(\mu\frac{\partial u}{\partial y}\right) + \rho g \tag{3}$$

y-component:

$$\rho\left(u\frac{\partial v}{\partial x} + v\frac{\partial v}{\partial y}\right) = -\frac{\partial P}{\partial y} + \frac{\partial}{\partial x}\left(\mu\frac{\partial v}{\partial x}\right) + \frac{\partial}{\partial y}\left(\mu\frac{\partial v}{\partial y}\right) \tag{4}$$

where P is the pressure, μ is the viscosity of the gas mixture, and g is the gravitational acceleration. The gravitational force is included in the momentum equation to predict natural convection effects.

The energy equation can be written as

$$\rho C_P\left(u\frac{\partial T}{\partial x} + v\frac{\partial T}{\partial y}\right) = \frac{\partial}{\partial x}\left(k\frac{\partial T}{\partial x}\right) + \frac{\partial}{\partial y}\left(k\frac{\partial T}{\partial y}\right) \tag{5}$$

where C_P and k are the heat capacity and thermal conductivity of the gas, respectively.

Finally, species balance equations take the form

$$C\left(u\frac{\partial x_i}{\partial x} + v\frac{\partial x_i}{\partial y}\right) = \frac{\partial}{\partial x}\left[CD_i\left(\frac{\partial x_i}{\partial x} + \alpha_i x_i \frac{\partial \ln T}{\partial x}\right)\right] + \frac{\partial}{\partial y}\left[CD_i\left(\frac{\partial x_i}{\partial y} + \alpha_i x_i \frac{\partial \ln T}{\partial y}\right)\right] + R_{g,i} \tag{6}$$

where C is the gas concentration, x_i is the mole fraction of species i, D_i is the multicomponent diffusion coefficient of species i, α_i is the multicomponent thermal diffusion factor of species i, and $R_{g,i}$ is the rate of formation of species i by gas phase reactions whose details are discussed in the Chemical Model section.

2. Boundary Conditions

Since the WJ 7000 CVD reactor is axisymmetric, computations are performed over half the chamber. Boundary conditions on the above set of transport equations should be specified at the inlet, outlet, symmetric axis, solid walls, and wa-

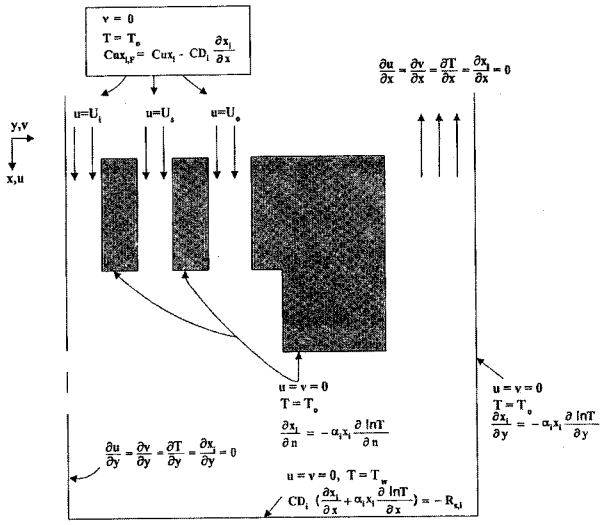

Fig. 2. Boundary conditions used for simulations.

fer surface as shown in Fig. 2. At the inlet, Danckwerts' conditions are used for the species balance [Danckwerts, 1953]. At the outlet, a zero normal gradient condition is applied for all dependent variables. On the solid walls, the normal and tangential velocities are zero, and no films are deposited because the reactor wall is cooled at T_o (=60 °C).

3. Chemical Model

Kinetic mechanisms for the TEOS/ozone process used in this work are described in detail by Kim and Gill [1994]. Details of gas phase and surface reactions are shown in Fig. 3. Murase et al. [1993] observed in their experiments that reaction byproducts in Fig. 3 are ethylene, water, and oxygen. According to Popovich et al. [1985], it is assumed that ozone decomposes after excitation by collisions with other species in the gas phase, the decomposition of excited ozone to oxygen atoms, and simultaneous generation of additional oxygen molecules through interaction of oxygen atoms with ozone. TEOS decomposes to intermediate, I, in the gas phase when reacting with excited ozone. Some of the intermediate molecules are consumed to useless products in the gas phase before they approach the wafer surface, thus implying parasitic gas phase reactions. Undecomposed intermediate molecules adsorb on the wafer surface, and then decompose to yield SiO_2 films. With steady-state assumptions for oxygen atoms and activated ozone, Kim and Gill [1994] determined the detailed rate expressions for the gas phase reactions and surface reactions as follows

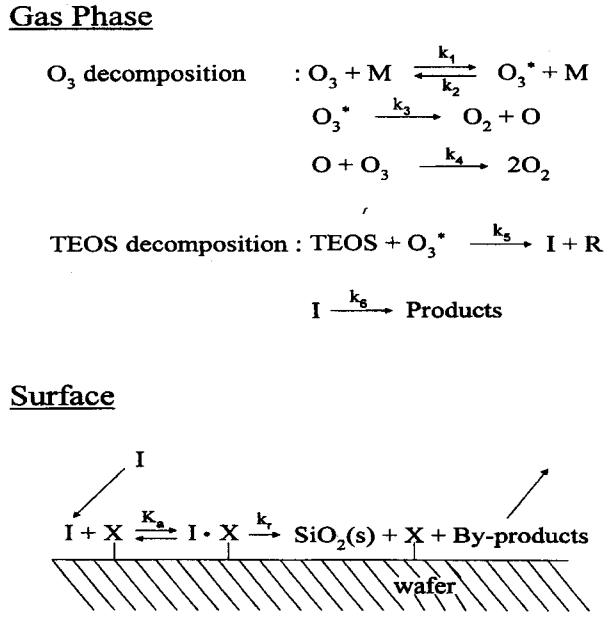

Fig. 3. Details of deposition mechanism for the TEOS-ozone CVD.

Gas phase

$$R_{g,O_3} = -k_{O_3} C_M C_{O_3} \tag{7}$$

$$R_{g,TEOS} = -k_{TEOS} C_M C_{O_3} C_{TEOS} \tag{8}$$

$$R_{g,I} = -k_{TEOS} C_M C_{O_3} C_{TEOS} - k_I C_I \tag{9}$$

where $k_{O_3} = 2k_1$, $k_{TEOS} = k_1 k_5 / k_3$, and $k_I = k_6$.

Surface

$$R_{S,I} = \frac{k_r K_a C_{I,W}}{1 + K_a C_{I,W}} \tag{10}$$

where k_r is the surface reaction rate constant, K_a is the equilibrium constant for adsorption, and $C_{I,W}$ is the concentration of intermediate at the wafer-gas interface. The rate constants for the gas phase reactions are given as

$$k_{O_3} = 7.0 \times 10^{15} e^{(-22{,}700/RT)} \quad cm^3 mol^{-1} s^{-1} \tag{11}$$

$$k_{TEOS} = 1.85 \times 10^{25} e^{(-28{,}000/RT)} \quad cm^6 mol^{-2} s^{-1} \tag{12}$$

$$k_I = 2.72 \times 10^{6} e^{(-11{,}100/RT)} \quad s^{-1} \tag{13}$$

The surface reaction rate and adsorption equilibrium constants, respectively, are

$$k_r = 1.29 \times 10^{-6} e^{(-2{,}930/RT)} \quad mol\ cm^{-2} s^{-1} \tag{14}$$

$$K_a = 1.14 \times 10^{10} e^{(-5{,}120/RT)} \quad cm^3 mol^{-1} \tag{15}$$

4. Method of Solution

To solve the above set of governing equations along with appropriate boundary conditions in two-dimensional rectangular coordinates, we employ control-volume-based finite difference methods. The computational domain is divided into a number of finite control volumes surrounding the grid points. We use a staggered grid system in which the velocity components are stored midway between adjacent grid nodes while all the other variables are stored at the grid nodes. The differential equations are integrated over discrete control volumes to generate the discretized equations. A power-law scheme is employed to evaluate the convection-diffusion fluxes. The continuity equation is coupled to the momentum equation through the SIMPLER (semi-implicit method for pressure-linked equations-revised) algorithm [Patankar, 1980]. The discretized equations resulting are coupled and nonlinear. A line-by-line method that is a combination of the tridiagonal-matrix algorithm (TDMA) and the Gauss-Seidel method is used to solve the discretized algebraic equations. The computational domain typically consists of 55 grid cells in the longitudinal direction and 120

grid cells in the lateral direction. The relative change from one iteration to the next for several particular monitor grid points and for each dependent variable has been checked and was typically less than 10^{-5} after 200 iterations. The error in the global mass balance for the total flow was on the order of 10^{-17}.

RESULTS AND DISCUSSION

Fig. 4 illustrates the effect of parasitic gas phase reactions at 60 torr in the AM 5000 in which the reactant gas mixture enters the chamber from the showerhead. In Fig. 4, the total flow rate is 3000 sccm and O_3/TEOS ratio is 2, which are typical operating conditions used in the AM 5000. The upper curve stands for a maximum deposition rate which can be obtainable theoretically if parasitic gas phase reactions are prevented. We see in Fig. 4 that as the temperature is increased from 280 to 405 °C, the difference in deposition rate, ΔR_d, is increased from 12 to 245 nm/min indicating that parasitic gas phase reactions become more significant with higher temperatures. Therefore, parasitic gas phase reactions, even at 60 torr, markedly reduce deposition rates and this effect becomes more considerable at higher pressures. This loss of deposition rate seems to be inevitable in such a configuration as the AM 5000 in which intimate gas phase mixing occurs. The WJ configuration attempts to address this problem. The TEOS and ozone streams injected into the WJ 7000 CVD chamber are separated by an inert gas "blanket" stream in order to diminish gas phase reactions which are highly severe at the atmospheric pressure.

In the AM 5000, the size of the showerhead is comparable to that of the wafer so that reactant mixture is distributed uniformly over the entire wafer surface leading to a uniform film. However, in the WJ 7000 the size of the injector is only a few mm; thus reactants are distributed over a relatively small portion of the wafer. Typical operating conditions for the WJ 7000 are listed in Table 1. Here flow rates in sccm for three ports correspond to the following linear velocities: inner-port velocity, U_i=25 cm/s, separator-port velocity, U_s=29 cm/s, outer-port velocity, U_o=31 cm/s, respectively. Note that the O_3/TEOS ratio employed in the WJ 7000 ranges from about 5 to 30, which is much higher than that in the AM 5000. Operating conditions shown in Table 1 are used as basic conditions for simulations performed in this work.

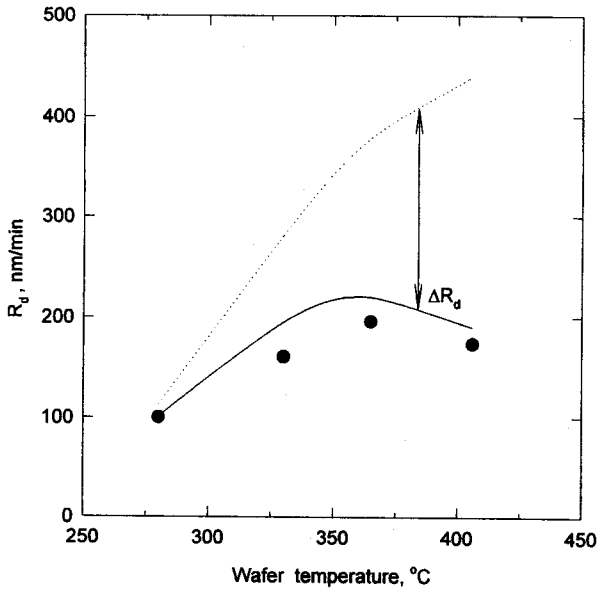

Fig. 4. Effect of parasitic gas phase reaction at 60 torr in the AM 5000. Experimental results (●) from Kim and Gill [1994]. Predicted results with (=solid line) and without (=dotted line) parasitic gas phase reaction.

Table 1. Typical operating conditions for the WJ 7000

Operating parameter		Value
Flow rate	Inner-port	3,150 sccm
	Separator-port	8,400 sccm
	Outer-port	7,400 sccm
	TEOS	15 sccm
	Ozone	70-500 sccm
Temperature	Injector	400 °C
	Wafer	60 °C
Pressure		760 torr
Gap spacing		12.5 mm

The simulated streamlines for the WJ APCVD chamber are shown in Fig. 5a for typical operating conditions given in Table 1. The values in Fig. 5a indicate the stream functions in g/cm-s. The predicted results show that no strong recirculations are generated between injector and wafer even though the WJ process is operated under atmospheric pressure where the natural convection effects may be pronounced. The recirculations appearing above the wafer must be avoided because they lead to a fatal result in film properties and uniformity. Generally, one can reduce these recirculations by increasing the flow rate and reducing the gap spacing [Kim and Gill, 1994]. It seems from Fig. 5a that the gas velocities and gap spacing used in the WJ operation are appropriate for preventing the recirculations. The computed temperature distributions are illustrated in Fig. 5b. We see in Fig. 5b that in the region near the center most of the gas phase temperature remains at 60 °C because of high injection velocities. The average gas phase temperature at the center is lower than that under the injector block. Therefore, the effect of parasitic gas phase reactions is more significant under the injector block than at the center of the chamber. This may result in a dramatic decrease in deposition rate as one moves away from the center.

Film thickness profiles on a stationary wafer called "static prints" are depicted in Fig. 6. We see that the resulting film forms a stripe that is the thickest directly under the injector, tailing off downstream. As mentioned above, the TEOS stream is separated from the ozone stream by the blanket nitrogen stream. TEOS alone, of course, cannot produce SiO_2 films at temperatures below 600 °C. As the gases exit from the injector slots, TEOS and ozone molecules are transferred in the counter region, respectively, by diffusion through a nitrogen blanket layer and produce intermediate species when colliding in the gas phase. One of interesting experimental results ob-

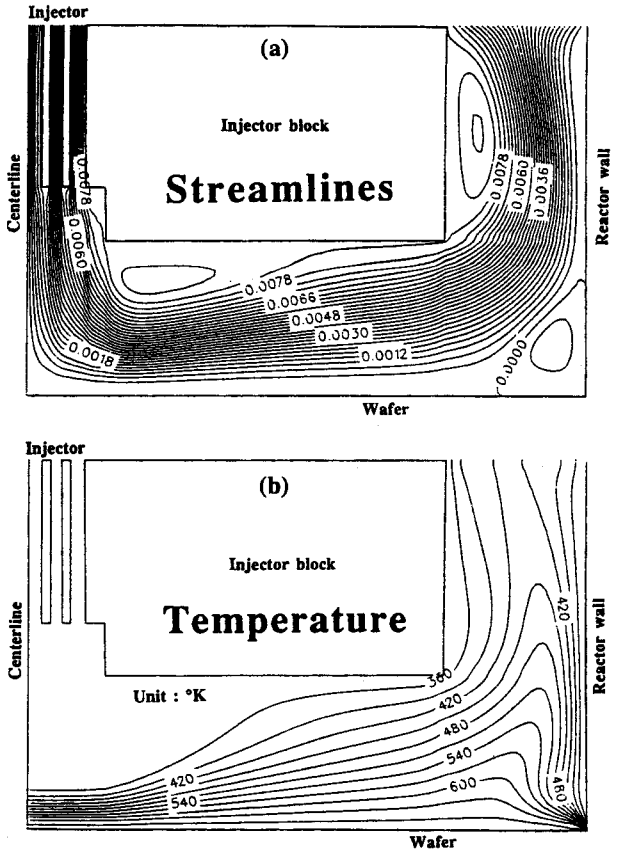

Fig. 5. Computed streamline and temperature distributions in the WJ 7000 chamber for typical operating conditions given in Table 1.

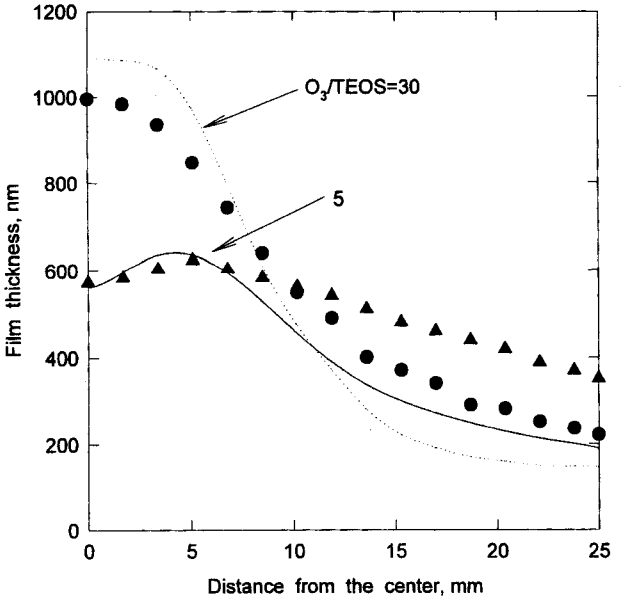

Fig. 6. Film thickness profiles on a stationary wafer depending on the O_3/TEOS ratio. The deposition time is 16 min. Experimental results for O_3/TEOS=5 (▲) and 30 (●) from Li et al. [1993]. Predicted results for O_3/TEOS=5 (solid line) and 30 (dotted line).

served in the WJ 7000 is that a local minimum in the film thickness occurs directly under the injector at a low O_3/TEOS ratio of 5 as shown in Fig. 6. This is because the intermediate species are insufficiently generated in the gas phase under the injector at a low ozone concentration. However, as the O_3/TEOS ratio is increased from 5 to 30, the intermediate species are then sufficiently generated in the center region due to a high ozone concentration leading to a film of central peak type. Note here that the film thickness decreases more sharply in the tail region at an O_3/TEOS ratio of 30 than at an O_3/TEOS ratio of 5. According to the kinetic mechanisms proposed by Kim and Gill [1994], high ozone concentrations promote parasitic gas phase reactions leading to a decrease in deposition rate. As seen in Fig. 6, the model successfully explains the behavior of experimental data. Actually, there is a nitrogen shield which nitrogen purges through in order to protect the injector and reactor wall from deposition and contamination [Dobkin, 1993]. However, detailed information on the nitrogen shield is not available, which does not enable us to include this effect in the model. This may account for a discrepancy between predicted results and experimental data especially in the tail region. We believe that including the nitrogen shield effect in the model will improve the predicted results because the ozone concentration is lowered when the reactants mix with the shielding nitrogen, thereby reducing parasitic gas phase reactions. During a commercial run the wafer is moving very slowly under the injector at a speed of about 0.08 cm/s, and the resulting film is very uniform. Typically the standard deviation of the mean thickness is 2% or less. Therefore, the film uniformity does not seem to be a critical issue in the WJ 7000 operation.

We now examine the effect of operating conditions on the average deposition rate across the wafer surface. In all calculations made in this study, the pressure is fixed at 760 torr because the WJ 7000 is operated under atmospheric pressure. Nishimoto et al. [1989] found in their TEOS/O_3 APCVD experiments that the deposition rate is decreased with increasing wafer temperature, whereas the film qualities such as etch rate, shrinkage and current leakage are remarkably improved. Therefore, there is a competition between the deposition rate and the film quality in the TEOS/O_3 APCVD process. The wafer temperature is typically maintained at 400 °C in the WJ 7000 operation, which produces good film qualities. Since it is required to obtain in the WJ 7000 both higher film growth rates and better film quality, the wafer temperature is also fixed at 400 °C in this work.

The dependence of deposition rate on inner-port velocity, U_i, is illustrated in Fig. 7a in which the separator-port velocity, U_s, is fixed at 29 cm/s. The deposition rates in Figs. 7-9 are the average ones across the wafer surface. It can be seen in Fig. 7a that the deposition rate increases dramatically from 30 nm/min to 250 nm/min as U_i is increased from 25 cm/s to 50 cm/s at U_o=31 cm/s. This suggests that the deposition rate is sensitive to small changes in U_i. The predicted results show the same trend for U_o=40 cm/s. As the inner-port velocity, e. g. total flow rate, is increased, the TEOS flow rate is increased, thus generating more intermediate species in the gas phase resulting in an increase in deposition rate. In addition, the

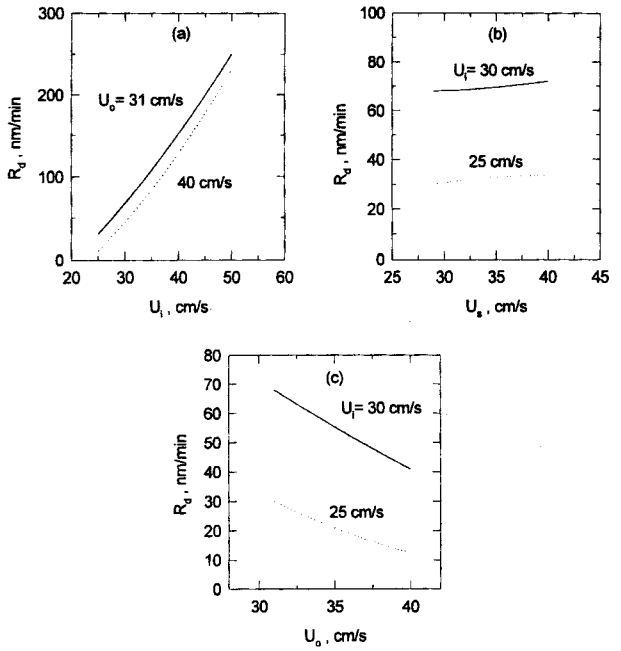

Fig. 7. Dependence of deposition rate on (a) inner-port velocity, U_i for U_s=29 cm/s; (b) separator-port velocity, U_s for U_o=31 cm/s; (c) outer-port velocity, U_o for U_s=29 cm/s.

convective transfer is enhanced as the total flow rate is increased. This effect may be favorable in generating intermediate species in the gas phase. Kim and Gill [1994] showed that in the AM 5000 the deposition rate is also increased with increasing TEOS flow rate. The dependence of deposition rate on separator-port velocity, U_s, is shown in Fig. 7b. Here U_o is fixed at 31 cm/s. We see that as one increases the separator-port velocity, U_s, from 29 cm/s to 40 cm/s at U_i=30 cm/s, the deposition rate increases slightly from 68 nm/min to 72 nm/min. Therefore, the deposition rate does not depend strongly on the separator-port velocity. An increase in U_s prevents the TEOS stream from mixing with the ozone stream. This reduces parasitic gas phase reactions. However, TEOS molecules colliding with ozone molecules are also reduced, generating less intermediate species. This may reflect a slight increase in deposition rate with U_s. Fig. 7c shows the influence of outer-port velocity, U_o, on deposition rate. Here U_s is fixed at 29 cm/s. If one increases U_o from 31 cm/s to 40 cm/s, the deposition rate decreases significantly from 68 nm/min to 41 nm/min at U_i=30 cm/s as shown in Fig. 7c. As the outer-port velocity is increased, the ozone flow rate is increased accelerating parasitic gas phase reactions. This results in a decrease in deposition rate, but the film quality may be improved because of higher ozone concentration. From the results above, the velocity at each port has a different effect on deposition rate.

Fig. 8 illustrates the effect of O_3/TEOS ratio on deposition rate for fixed port velocities. One can see in Fig. 8 that the deposition rate increases with O_3/TEOS ratio up to about 30 at which a maximum occurs, and it decreases with further increasing O_3/TEOS ratio. At low O_3/TEOS ratios below 30, the deposition rate increases with increasing O_3/TEOS ratio

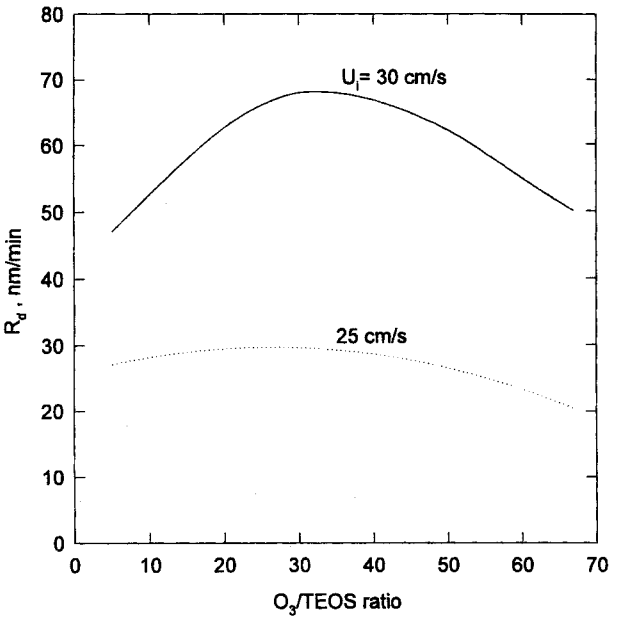

Fig. 8. Dependence of deposition rate on O_3/TEOS ratio. U_s= 29 cm/s and U_o=31 cm/s.

because more intermediate species are generated in the gas phase. However, at high O_3/TEOS ratios above 30, high ozone concentration promotes parasitic gas phase reactions leading to a decrease in deposition rate. This behavior becomes pronounced as the inner-port velocity, U_i, is increased from 25 cm/s to 30 cm/s. Note that a very high O_3/TEOS ratio where the film quality is excellent is feasible in the WJ operation without reducing deposition rate, unlike the AM 5000 in which the O_3/TEOS ratio typically increases up to 10.

Finally, Fig. 9 shows the dependence of deposition rate on gap spacing between injector and wafer. As the gap spacing

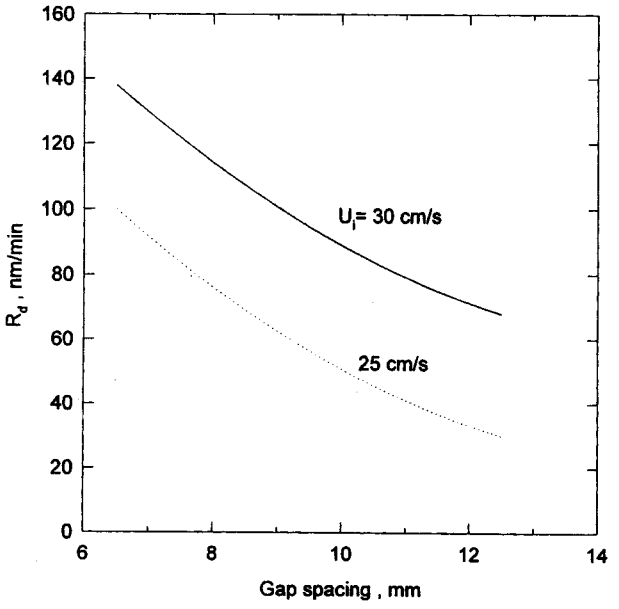

Fig. 9. Dependence of deposition rate on gap spacing. U_s=29 cm/s and U_o=31 cm/s.

is increased from 7 mm to 12.5 mm, the deposition rate monotonically decreases from 138 nm/min to 68 nm/min at U_i= 30 cm/s. As the gap spacing increases, the residence time of the molecules in the reactor increases for a given flow rate and thus the intermediate species are depleted in the gas phase due to significant parasitic gas phase reactions in APCVD. Therefore, one can increase deposition rate with decreasing gap spacing. However, as the gap spacing is decreased the ozone concentration near the wafer center is reduced deteriorating the film quality. This may need a further study combined with experiments.

CONCLUSIONS

In this work, we have developed a mathematical model to study the CVD of SiO_2 from TEOS and ozone in a cold-wall separate-gas-injection reactor related to the commercial WJ 7000. The model successfully explains experimental data of film thickness profiles on a stationary wafer showing a narrow central peak. The WJ 7000 configuration is found to be effective in reducing parasitic gas phase reactions in the TEOS/ozone APCVD process. We investigate the effect of operating conditions on deposition rate. The predicted results show that the deposition rate:

1. increases markedly with increasing inner-port velocity.
2. increases slightly with increasing separator-port velocity.
3. decreases with increasing outer-port velocity.
4. becomes a maximum at O_3/TEOS ratio of about 30.
5. decreases with increasing gap spacing.

In conclusion, a high TEOS flow rate and a high O_3/TEOS ratio of 30 are preferable in obtaining high deposition rates and good film quality in the WJ 7000 operation.

ACKNOWLEDGMENT

This work was supported financially by the University of Ulsan under a 1997 University Research Grant.

NOMENCLATURE

C : gas concentration [mol/cm^3]
C_p : heat capacity of the gas [cal/g-K]
D_i : diffusion coefficient of species i [cm^2/s]
g : acceleration of gravity [=980 cm/s^2]
k : thermal conductivity of the gas [cal/cm-K]
K_a : adsorption equilibrium constant [cm^3/mol]
k_r : surface reaction rate constant [mol/cm^2-s]
P : absolute pressure [dyne/cm^2]
R : gas constant [=1.987 cal/mol-K]
$R_{g,i}$: rate of formation of species i by gas-phase reactions [mol/cm^3-s]
$R_{s,i}$: rate of formation of species i by surface reactions [mol/cm^2-s]
T : absolute temperature [K]
u : longitudinal velocity [cm/s]
U : linear velocity at the port [cm/s]
v : lateral velocity [cm/s]
x : longitudinal coordinate
x_i : mole fraction of species i
y : lateral coordinate

Greek Letters

α_i : thermal diffusion factor of species i
μ : gas viscosity [g/cm-s]
ρ : gas density [g/cm^3]
Ψ : stream function [g/cm-s]

REFERENCES

Chin, B. L. and Van de Ven, E. P., "Plasma TEOS Process for Interlayer Dielectric Applications", *Solid State Technology*, **April**, 119 (1988).

Danckwerts, P. V., "Continuous Flow System: Distribution of Residence Times", *Chem. Eng. Sci.*, **2**, 1 (1953).

Dobkin, D. with Watkins-Johnson, Private communication, 1993.

Fujino, K., Nishimoto, Y., Tokumasu, N. and Maeda, K., "Silicon Dioxide Deposition by Atmospheric Pressure and Low-Temperature CVD Using TEOS and Ozone", *J. Electrochem. Soc.*, **137**, 2883 (1990).

Ikeda, Y., Numasawa, Y. and Sakamoto, M., "Ozone/Organic-Source APCVD for Conformal Doped Oxide Films", *J. Electron. Mater.*, **19**, 45 (1990).

Jeon, B.-J., Oh, I.-H., Lim, T.-H. and Jung, I.-H., "Characteristics of Silicon Oxide Films Prepared by Chemical Vapor Deposition Using ECR Plasma Source", *HWAHAK KONGHAK*, **35**, 374 (1997).

Kim, E. J. and Gill, W. N., "A New Model for Low Pressure Chemical Vapor Deposition of SiO_2 Films by Ozone Augmented Tetraethoxysilane", *J. Crystal Growth*, **140**, 308 (1994): "Analytical Model for Chemical Vapor Deposition of SiO_2 Films Using Tetraethoxysilane and Ozone", *J. Crystal Growth*, **140**, 315 (1994): "Modeling of CVD of Silicon Dioxide Using TEOS and Ozone in a Single-Wafer Reactor", *J. Electrochem. Soc.*, **141**, 3462 (1994).

Li, J., McVittie, J. P., Ferziger, J. H. and Saraswat, K. C., "Profile Simulation of APCVD Oxide from Ozone TEOS", Techcon'93, 463, Sep. 28-30 (1993).

Murase, K., Yabumoto, N. and Komine, Y., "Thermal Desorption Studies of Silicon Dioxide Deposited by Atmospheric-Pressure Chemical Vapor Deposition Using Tetraethylorthosilicate and Ozone", *J. Electrochem. Soc.*, **140**, 1722 (1993).

Nguyen, S., Dobuzinsky, D., Harmon, D., Gleason, R. and Fridman, S., "Reaction Mechanisms of Plasma- and Thermal Assisted Chemical Vapor Deposition of Tetraethylorthosilicate Oxide", *J. Electrochem. Soc.*, **137**, 2209 (1990).

Nishimoto, Y., Tokumasu, N., Fujino, K. and Maeda, K., "Dielectric Film Deposition by Atmospheric Pressure and Low Temperature", IEEE VMIC Conference, 382, June 12-13 (1989).

Park, Y.-B., Kang, J.-K. and Rhee, S.-W., "Remote Plasma

Chemical Vapor Deposition (RPCVD) of Low Temperature Silicon Oxide", *HWAHAK KONGHAK*, **34**, 143 (1996).
Patankar, S. V., "Numerical Heat Transfer and Fluid Flow", Hemisphere Publishing Corp., Washington, DC (1980).
Popovich, M. O., Egorova, G. V. and Filippov, Yu. V., "Low-temperature Pyrolysis of Ozone", *Russ. J. Phys. Chem.*, **59**, 165 (1985).
Shareef, I. A., Rubloff, G. W., Anderle, M., Gill, W. N., Cotte, J. and Kim, D. H., "Subatmospheric Chemical Vapor Deposition Ozone/TEOS Process for SiO_2 Trench Filling", *J. Vac. Sci. Technol. B*, **13**, 1888 (1995).